Comparison of Turbulence Models for Computational Fluid Dynamics Simulation of Wind Flow on Cluster of Buildings in Mandalay

Thet Mon Soe[*], San Yu Khaing[**]

[*] Department of Civil Engineering, Mandalay Technological University
[**] Department of Civil Engineering, Mandalay Technological University

Abstract- CFD (Computational Fluid Dynamics) simulation is the main research method for assessing the wind environment around building complexes. In this paper, a comparison of different turbulence models in simulating wind environment around building complexes is conducted to discuss their precision of simulation. Present work used a three dimensional scale down model of buildings where steady flow analysis has been done. It has been implemented through ANSYS Fluent 17.0 using SIMPLE algorithm as solver. The turbulence models used as the RANS based model: the standard k-epsilon model, RNG k-epsilon model and Realizable k- ε model. Firstly, the CFD simulation results for single high rise building showed good agreement of approximately 99% in Cp compared to the experimental results obtained from Tokyo Polytechnic University "New frontier of Education and Research in Wind Engineering". Secondly, the CFD simulation results for the surrounding effect of building are investigated. The effects of the surroundings significantly reduce the surface pressure coefficients. Thirdly, For the existing cluster of building in Mandalay, Wind pressure coefficients are compared with the three different turbulence models in Fluent. The Standard k-ε model and Realizable k-ε model appear to produce exactly prediction wake recirculation zone. The RNG k-ε model greatly over predicts the size of the recirculation zone and a strong wake flow among buildings. The standard k-ε, RNG k-ε, realizable k-ε models produce similarly shaped contour map of pressure but with significant differences in magnitude.

Index Terms- Computational Fluid Dynamics; RANS; Single High Rise Building; Surrounding Effect; Existing Cluster Of Building.

I. INTRODUCTION

Wind is an important issue on high-rise buildings. Wind causes aerodynamic pressures on the surfaces of the buildings. These wind induced aerodynamic pressures also vary randomly with time and space. There is a huge demand for high rise buildings in developing countries and developed countries. With the development in technology taller and taller structures are being designed and constructed to care of the local need and desire. Such structures have a significant effect on the surrounding wind patterns. High rise buildings in urban areas should be designed to ensure comfort of their inhabitants and users. The construction of a building inevitably changes the outdoor environment around the building. These changes include wind speed, wind direction, air pollution, driving rain and heat radiation. The change of these quantities depends on the shape, size and orientation of the building and on the interdependence of the buildings with surrounding buildings. This causes many environmental problems in nearby areas such as accelerated wind flow at the ground level impacting the comfort, and sometimes safety, of the users of the building and the pedestrians in the surrounding street canyons. For a safe structural design of any particular structure, it is necessary to consider wind effects. Although one cannot see the wind, it is a common observation that its flow is quite complex and turbulent in nature and has a tendency to exert differential velocity and pressure field around any obstacle likely to obstruct its flow path. The generalized estimation of wind loading is carried out by defining pressure coefficients. Pressure coefficients are non-dimensional parameter which is used to assess magnitude. Pressure coefficients are influenced by various parameters like, shape, structural geometry, incident wind profile, terrain roughness, turbulence in the wind, location of a particular structure etc [1].

Modelling the wind atmosphere associated with proposed or existing buildings is of great importance for the wind engineering, Civil Construction sectors as well as Structural Engineering Sectors. Computational Wind Engineering (CWE) as a branch of Computational Fluid Dynamics (CFD) has been developed rapidly over the last three decades to evaluate the interaction Computational Fluid Dynamics (CFD) simulations are being widely used by engineers for various wind engineering studies such as determine wind loads on buildings, evaluating wind flow patterns in built areas, predicting pollutants depression patterns in urban areas, evaluate pedestrian level wind comforts, etc. CFD (Computational Fluid Dynamics) simulation methods are employed as the main methods for studying the outdoor wind environment today. The precision of simulation results is influenced by many factors, such as algorithms, boundary conditions and turbulence models.

Due to the time and cost issues involved in wind tunnel testing, CFD is now widely employed for the prediction of flow fields. The first CFD techniques were introduced in the early 1950s, made possible by the advent of the digital computer [Chung, 2002]. CFD is a computer-based mathematical modeling tool capable of dealing with fluid flow problems and predicting physical fluid flows and heat transfer [2]. While traditionally thought of as exclusively for use in aerodynamic research, CFD analysis is now being applied in many

other fields, including marine engineering, electrical and electronic engineering, biomedical engineering, chemical engineering, environmental engineering, wind engineering, hydrology, oceanography, meteorology, and nuclear power [2].
In this journal, the wind pressure characteristics are investigated with the following three cases:
(1) A single high rise building case is first considered with three different turbulence models and is compared with the experimental results obtained from Tokyo Polytechnic University "New frontier of Education and Research in Wind Engineering", to explain the method used to validate our CFD simulations.
(2) And then, a high rise building with surrounding buildings cases are investigated to predict wind characteristics of the flow field.
(3) Finally, existing cluster of buildings case is considered with CFD simulation by using ANSYS Fluent to predict wind pressure coefficients and wind pressure distributions with height on the L-shape building and to investigate the flow path of the velocity distributions within actual existing cluster of buildings in Mandalay.

II. METHODOLOGY

When performing a simulation, the user typically chooses target variables, the approximate form of the governing equations, the turbulence model, the level of detail in the geometrical representation of the buildings, the size of the computational domain, the type and resolution of the computational grid, the boundary conditions, the discretization schemes, and the iterative convergence criteria.

A. Computational Fluid Dynamics

Modeling the wind atmosphere associated with proposed or existing buildings is of great importance for the wind engineering, Civil Construction sectors as well as Structural Engineering Sectors. Computational Wind Engineering (CWE) as a branch of Computational Fluid Dynamics (CFD) has been developed rapidly over the last three decades to evaluate the interaction Computational Fluid Dynamics (CFD) simulations are being widely used by engineers for various wind engineering studies such as determine wind loads on buildings, evaluating wind flow patterns in built areas, predicting pollutants depression patterns in urban areas, evaluate pedestrian level wind comforts, etc. Numerical simulations are more flexible and robust in terms of simulating wind flow conditions together with detailed surrounding features such as buildings, mountains, tree, etc. CFD techniques have been adopted for the estimation of wind flow around building. Progress in high-speed processing by personal computer and rapid propagation of software for numerical analysis of fluid dynamics in recent years have enabled prediction of the pedestrian wind environment around high-rise buildings based on CFD. CFD simulations would be a smart tool for practicing engineers to analyses wind conditions in vicinity of a high-rise building.
In Myanmar, wind engineering is not as much as developed compared the other branches of civil engineering. Nowadays, the concern of wind engineering is increasing among Myanmar engineers due to increase of damages due to frequent occurrence of high wind events and construction of many high-rise buildings in city center, which are more susceptible to wind load. Environmentally, wind, sunlight, natural light, air, noise, skyline, landscape and traffic are the major physical factors that are affected from high-rise existence. These parameters affect quality of life and the conditions under which people live and work. The use of natural ventilation is highly constrained by its surrounding environments. The sheltering effect of the surrounding built-up environment can reduce pressure differences across a building which is necessary to produce adequate ventilation rates.
Computational Fluid Dynamics (CFD) represents the science and methodology of predicting fluid flow by solving governing equations using a numerical algorithm and necessary empirical models. CFD was made possible with the advent of the computer and is continually benefited by increased processor speeds and memory allowance. There are three main components to the implementation of CFD methodology: grid generation, algorithm development, and turbulence / empirical modeling. Grid generation refers to segregating the flow domain into individual cells or elements. The grid is used to calculate derivatives and fluxes for the numerical algorithm. The numerical algorithm refers to how the derivatives and fluxes are calculated i.e. central differenced or up-winded and order of accuracy etc. Models are used to reduce computational requirements (such as processor speed and memory) involved in resolving turbulent flow.

B. Governing equations

Wind engineers study more about the lower part of the atmosphere though entire earth atmosphere extends few kilometers above the earth surface. This lower part of the atmosphere is called as atmospheric boundary layer (ABL), which is directly under influence of earth surface itself such as shape, friction, thermal with time scales of less than a day and turbulent motion length scales of the order of boundary layer depth [3]. This boundary layer depth can be varying from several hundred meters to more than a kilometer aloft. Thus, most of manmade structures are well within the atmospheric boundary layer, governing flow equations can apply in this layer easily. However, both time and length scales of atmospheric flows have large variations. Thus, numerical simulations are divided in to micro-scale and meso-scale based on time and length scale for easiness of study. In this study, term CFD simulation is strictly used to describe the simulation of smaller length (~10 cm - 100 m) and time scales (~1 minute – 1 hour), thus probably in the category of micro-scale modelling. Most of governing equations in fluid dynamics can be applied to the atmospheric flows. The main governing equations are about conservation of mass (equation 1) and momentum (equation 2). The latter is also known as Navier-Stokes equation for motion of the fluid.

$$\frac{\partial \rho}{\partial t} + \frac{\partial (\rho u_i)}{\partial x_i} = 0 \quad (1)$$

$$\frac{\partial \rho u_i}{\partial t} + \frac{\partial (\rho u_i u_j)}{\partial x_j} = \frac{\partial P}{\partial x_i} + \frac{\partial}{\partial x_j}\left[\mu \left(\frac{\partial u_i}{\partial x_j} + \frac{\partial u_j}{\partial x_i} \right) \right] \quad (2)$$

Where, ui, uj are velocity components, ρ is air density, P is air pressure, μ is dynamic viscosity, and t is time. In this equation, Coriolis force and buoyance force are not considered as their effect is negligible in smaller length and time scale, which is valid for micro-scale CFD simulations.

C. Turbulence Models

Turbulence modeling is the computational procedure to solve and analyze the fluid flow introducing some approximations in the governing differential equations so that required solution is obtained approximately consuming feasible computational memory and time. Turbulence modeling is based on the assumption that the real flow field may be substituted by an imaginary field of mathematically defined continuous functions. The objective of the turbulence modeling is to develop a set of constitutive relations valid for any general turbulent flow problem which yield sufficiently reliable predictions and offer a degree of universality sufficient to justify their usage in terms of computational effort and accuracy. Many turbulence modeling techniques deal with an approximation to the Navier-Stokes equations in form of averaging the different ranges of turbulent eddy scales. For prediction of turbulent flows, the available approaches of turbulence modeling are (i) Direct Numerical Simulation (DNS) (ii) Large Eddy Simulation (LES) (iii) Reynolds Averaged Navier Stokes solution (RANS). The most common approach in CWE is RANS. Therefore, this section focuses on the turbulence models used in RANS. The equations of the RANS models calculate the transport equations only for the average quantities of the air flow, for which all the turbulence scales are simulated. By the early 1950's, four main categories of turbulence models had developed:

(1) Algebraic (Zero-Equation) Models
(2) One-Equation Models
(3) Two-Equation Models
(4) Second-Order Closure Models

With increased computer capabilities beginning in the 1960's, further development of all four of these classes of turbulence models has occurred.

Among them, Two-equation models have been the most popular models for a wide range of engineering analysis and research. These models provide independent transport equations for both the turbulence length scale, or some equivalent parameter, and the turbulent kinetic energy. With the specification of these two variables, two-equation models are complete; no additional information about the turbulence is necessary to use the model for a given flow scenario. While this is encouraging in that these models may appear to apply to a wide range of flows, it is instructive to understand the implicit assumptions made in formulating a two-equation model. Specifically, most two-equation models make the same fundamental assumption of local equilibrium, where turbulent production and dissipation balance. This assumption further implies that the scales of the turbulence are locally proportional to the scales of the mean flow; therefore, most two equation models will be in error when applied to non-equilibrium flows. Though somewhat restricted, two-equation models are still very popular and can be used to give results well within engineering accuracy when applied to appropriate cases [4].

The K-epsilon model is one of the most common turbulence models. It is a two equation model, which means, it includes two extra transport equations to represent the turbulent properties of the flow. This allows a two equation model to account for history effects like convection and diffusion of turbulent energy. The first transported variable is turbulent kinetic energy, k. The second transported variable in this case is the turbulent dissipation, ε. It is the variable that determines the scale of the turbulence, whereas the first variable, k, determines the energy in the turbulence. To calculate boundary conditions for K-epsilon models see turbulence free-stream boundary conditions are;

(1) Standard k-epsilon model
(2) Standard k-epsilon hybrid model
(3) Realizable k-epsilon model
(4) Realizable k-epsilon hybrid model
(5) RNG k-epsilon model
(6) RNG k-epsilon hybrid model

In this study, models have been selected for numerical simulation for wind load prediction using three different turbulence models which are standard k-ε model, RNG k-ε model and Realizable k- ε model.

(1) Standard k- ε Model

Two-equation turbulence models allow the determination of both, a turbulent length and time scale by solving two separate transport equations. The standard k - ε model in ANSYS FLUENT falls within this class of models and has become the workhorse of practical engineering flow calculations in the time since it was proposed by Launder and Spalding. Robustness, economy, and reasonable

accuracy for a wide range of turbulent flows explain its popularity in industrial flow and heat transfer simulations. It is a semi-empirical model, and the derivation of the model equations relies on phenomenological considerations and empiricism.
The standard k - ε model is a model based on model transport equations for the turbulence kinetic energy (k) and its dissipation rate (ε). The model transport equation for k is derived from the exact equation, while the model transport equation for ε was obtained using physical reasoning and bears little resemblance to its mathematically exact counterpart.
In the derivation of the k-ε model, the assumption is that the flow is fully turbulent, and the effects of molecular viscosity are negligible. The standard k - ε model is therefore valid only for fully turbulent flows.
As the strengths and weaknesses of the standard k-ε model have become known, modifications have been introduced to improve its performance. Two of these variants are available in ANSYS FLUENT: the RNG k -ε model and the realizable k-ε model.
The turbulence kinetic energy, k, and its rate of dissipation, ε, are obtained from the following transport equations:

$$\frac{\partial}{\partial t}(\rho k)+\frac{\partial}{\partial x_i}(\rho k u_i)=\frac{\partial}{\partial x_j}\left[\left(\mu+\frac{\mu_t}{\sigma_k}\right)\frac{\partial k}{\partial x_j}\right]+G_k+G_b-\rho\varepsilon-Y_M+S_k \tag{3}$$

and

$$\frac{\partial}{\partial t}(\rho\varepsilon)+\frac{\partial}{\partial x_i}(\rho\varepsilon u_i)=\frac{\partial}{\partial x_j}\left[\left(\mu+\frac{\mu_t}{\sigma_\varepsilon}\right)\frac{\partial \varepsilon}{\partial x_j}\right]+C_{1\varepsilon}\frac{\varepsilon}{k}(G_k+C_{3\varepsilon}G_b)-C_{2\varepsilon}\rho\frac{\varepsilon^2}{k}+S_\varepsilon \tag{4}$$

In these equations, G_k represents the generation of turbulence kinetic energy due to the mean velocity gradients, calculated as described in Modeling Turbulent Production in the k- ε Models. G_b is the generation of turbulence kinetic energy due to buoyancy, calculated as described in Effects of Buoyancy on Turbulence in the k- ε Models. Y_M represents the contribution of the fluctuating dilatation in compressible turbulence to the overall dissipation rate, calculated as described in Effects of Compressibility on Turbulence in the k- ε Models. $C_{1\varepsilon}$, $C_{2\varepsilon}$, and $C_{3\varepsilon}$ are constants. σ_k and σ_ε are the turbulent Prandtl numbers for k and ε, respectively. S_k and S_ε are user-defined source terms.
The turbulent (or eddy) viscosity, μ_t, is computed by combining k and ε as follows:

$$\mu_t=\rho C_\mu\frac{k^2}{\varepsilon} \tag{5}$$

Where, C_μ is a constant
The model constants $C_{1\varepsilon}$, $C_{2\varepsilon}$, C_μ, σ_k and σ_ε have the following default values: $C_{1\varepsilon}$=1.44, $C_{2\varepsilon}$=1.92, C_μ=0.09, σ_k =1.0and σ_ε =1.3.

(2) RNG k- ε Model

The RNG k–ε model was derived using a statistical technique called renormalization group theory. It is similar in form to the standard k- ε model, but includes the following refinements:
(a) The RNG model has an additional term in its ε equation that improves the accuracy for rapidly strained flows.
(b) The effect of swirl on turbulence is included in the RNG model, enhancing accuracy for swirling flows.
(c) The RNG theory provides an analytical formula for turbulent Prandtl numbers, while the standard k- ε model uses user-specified, constant values.
The RNG-based k-ε turbulence model is derived from the instantaneous Navier-Stokes equations, using a mathematical technique called "renormalization group" (RNG) methods. The analytical derivation results in a model with constants different from those in the standard k - ε model, and additional terms and functions in the transport equations for k and ε.

The RNG k-ε model has a similar form to the standard k-ε model:

$$\frac{\partial}{\partial t}(\rho k)+\frac{\partial}{\partial x_i}(\rho k u_i)=\frac{\partial}{\partial x_j}\left[\alpha_k\mu_{eff}\frac{\partial k}{\partial x_j}\right]+G_k+G_b-\rho\varepsilon-Y_M+S_k \tag{6}$$

and

$$\frac{\partial}{\partial t}(\rho\varepsilon)+\frac{\partial}{\partial x_i}(\rho\varepsilon u_i)=\frac{\partial}{\partial x_j}\left[\alpha_\varepsilon\mu_{eff}\frac{\partial \varepsilon}{\partial x_j}\right]+C_{1\varepsilon}\frac{\varepsilon}{k}(G_k+C_{3\varepsilon}G_b)-C_{2\varepsilon}\rho\frac{\varepsilon^2}{k}-R_\varepsilon+S_\varepsilon \tag{7}$$

In these equations, G_k represents the generation of turbulence kinetic energy due to the mean velocity gradients, calculated as described in Modeling Turbulent Production in the k- ε Models. G_b is the generation of turbulence kinetic energy due to buoyancy, calculated as described in Effects of Buoyancy on Turbulence in the k- ε Models. Y_M represents the contribution of the fluctuating dilatation in compressible turbulence to the overall dissipation rate, calculated as described in Effects of Compressibility on Turbulence in the k- ε Models. $C_{1\varepsilon}$, $C_{2\varepsilon}$, and $C_{3\varepsilon}$ are constants. The quantities α_k and α_ε are the turbulent Prandtl numbers for k and ε, respectively. S_k and S_ε are user-defined source terms.
The scale elimination procedure in RNG theory results in a differential equation for turbulent viscosity:

$$d\left(\frac{\rho 2k}{\sqrt{\varepsilon\mu}}\right) = 1.72\frac{\hat{v}}{\sqrt{\hat{v}^3 - 1 + C_v}}d\hat{v} \quad (8)$$

Where;

$$\hat{v} = \frac{\mu_{eff}}{\mu} \quad , \quad C_v \approx 100$$

Equation 8 is integrated to obtain an accurate description of how the effective turbulent transport varies with the effective Reynolds number (or eddy scale), allowing the model to better handle low-Reynolds number and near-wall flows.
In the high-Reynolds number limit, Equation 8 gives

$$\mu_t = \rho C\mu\frac{k^2}{\varepsilon}$$

With C_μ = 0.0845, derived using RNG theory. It is interesting to note that this value of C_μ is very close to the empirically-determined value of 0.09 used in the standard k - ε model.
The inverse effective Prandtl numbers, α_k and α_ε are computed using the following formula derived analytically by the RNG theory:

$$\left|\frac{\alpha - 1.3929}{\alpha_0 - 1.3929}\right|^{0.6321}\left|\frac{\alpha + 2.3929}{\alpha_0 + 2.3929}\right|^{0.3679} = \frac{\mu_{mol}}{\mu_{eff}} \quad (9)$$

Where, α_0 =1.0. In the high-Reynolds number limit ($\frac{\mu mol}{\mu eff}$ = 1), $\alpha_k = \alpha_\varepsilon \approx 1.393$.

The main difference between the RNG and standard k -ε models lies in the additional term in the equation given by

$$R_\varepsilon = \frac{C_\mu\rho\eta^3\left(1 - \frac{\eta}{\eta_0}\right)}{1 + \beta\eta^3}\frac{\varepsilon^2}{k} \quad (10)$$

Where, $\eta \equiv \frac{Sk}{\varepsilon}$, η_0=4.38, β=0.012 .

The effects of this term in the RNG ε equation can be seen more clearly by rearranging Equation 7. Using Equation 10, the third and fourth terms on the right-hand side of Equation 7 can be merged, and the resulting equation can be rewritten as

$$\frac{\partial}{\partial t}(\rho\varepsilon) + \frac{\partial}{\partial x_i}(\rho\varepsilon u_i) = \frac{\partial}{\partial x_j}\left[\alpha_\varepsilon\mu_{eff}\frac{\partial\varepsilon}{\partial x_j}\right] + C_{1\varepsilon}\frac{\varepsilon}{k}(G_k + C_{3\varepsilon}G_b) - C_{2\varepsilon}^*\rho\frac{\varepsilon^2}{k} \quad (11)$$

Where, $C_{2\varepsilon}^*$ is given by

$$C_{2\varepsilon}^* \equiv C_{2\varepsilon} + \frac{C_\mu\eta^3\left(1 - \frac{\eta}{\eta_0}\right)}{1 + \beta\eta^3} \quad (12)$$

In regions where $\eta\langle\eta_0$, the R term makes a positive contribution, and $C_{2\varepsilon}^*$ becomes larger than $C_{2\varepsilon}$. In the logarithmic layer, for instance, it can be shown that η ≈ 3.0, giving $C_{2\varepsilon}^* \approx 2.0$, which is close in magnitude to the value of $C_{2\varepsilon}$ in the standard k-ε model (1.92). As a result, for weakly to moderately strained flows, the RNG model tends to give results largely comparable to the standard k -ε model.

In regions of large strain rate ($\eta\rangle\eta_0$), however, the R term makes a negative contribution, making the value of $C_{2\varepsilon}^*$ less than $C_{2\varepsilon}$.In comparison with the standard k-ε model, the smaller destruction of ε augments ε , reducing k and, eventually, the effective viscosity. As a result, in rapidly strained flows, the RNG model yields a lower turbulent viscosity than the standard k-ε model.

The model constants $C_{2\varepsilon}^*$ and $C_{2\varepsilon}$ in Equation 7 have values derived analytically by the RNG theory. These values, used by default in ANSYS FLUENT, are constants $C_{1\varepsilon}$ = 1.42, $C_{2\varepsilon}$ = 1.68.

(3) Realizable k- ε Model

The realizable k-ε model differs from the standard k-ε model in two important ways:
(a) The realizable k-ε model contains an alternative formulation for the turbulent viscosity.
(b) A modified transport equation for the dissipation rate, ε, has been derived from an exact equation for the transport of the mean-square vorticity fluctuation.

The term "realizable" means that the model satisfies certain mathematical constraints on the Reynolds stresses, consistent with the physics of turbulent flows. Neither the standard k-ε model nor the RNG k-ε model is realizable.
The realizable k-ε model proposed by Shih et al was intended to address these deficiencies of traditional k-ε models by adopting the following:
(a) A new eddy-viscosity formula involving a variable originally proposed by Reynolds.
(b) A new model equation for dissipation (ε) based on the dynamic equation of the mean-square vorticity fluctuation.
The modeled transport equations for k and ε in the realizable k-ε model are

$$\frac{\partial}{\partial t}(\rho k)+\frac{\partial}{\partial x_j}(\rho k u_i)=\frac{\partial}{\partial x_j}\left[\left(\mu+\frac{\mu_t}{\sigma_k}\right)\frac{\partial k}{\partial x_j}\right]+G_k+G_b-\rho\varepsilon-Y_M+S_k \tag{13}$$

and

$$\frac{\partial}{\partial t}(\rho\varepsilon)+\frac{\partial}{\partial x_i}(\rho\varepsilon u_i)=\frac{\partial}{\partial x_j}\left[\left(\mu+\frac{\mu_t}{\sigma_\varepsilon}\right)\frac{\partial \varepsilon}{\partial x_j}\right]+\rho C_1 S\varepsilon-\rho C_2\frac{\varepsilon^2}{k+\sqrt{\nu\varepsilon}}+C_{1\varepsilon}\frac{\varepsilon}{k}C_{3\varepsilon}G_b+S_\varepsilon \tag{14}$$

Where,

$$C_1=\max\left[0.43,\frac{\eta}{\eta+5}\right],\eta=S\frac{k}{\varepsilon},S=\sqrt{2S_{ij}S_{ij}}$$

In these equations, G_k represents the generation of turbulence kinetic energy due to the mean velocity gradients, calculated as described in Modeling Turbulent Production in the k- ε Models. G_b is the generation of turbulence kinetic energy due to buoyancy, calculated as described in Effects of Buoyancy on Turbulence in the k- ε Models. Y_M represents the contribution of the fluctuating dilatation in compressible turbulence to the overall dissipation rate, calculated as described in Effects of Compressibility on Turbulence in the k- ε Models. C_2 and $C_{2\varepsilon}$ are constants. σ_k and σ_ε are the turbulent Prandtl numbers for k and ε, respectively. S_k and S_ε are user-defined source terms.
As in other *k -ε* models, the eddy viscosity is computed from

$$\mu_t=\rho C_\mu\frac{k^2}{\varepsilon} \tag{15}$$

The difference between the realizable *k-ε* model and the standard and RNG *k- ε* models is that C_μ is no longer constant. It is computed from

$$C_\mu=\frac{1}{A_0+A_s\frac{ku^*}{\varepsilon}} \tag{16}$$

Where,

$$U^*\equiv\sqrt{S_{ij}S_{ij}+\tilde{\Omega}_{ij}\tilde{\Omega}_{ij}} \tag{17}$$

and

$$\tilde{\Omega}_{ij}=\Omega_{ij}-2\varepsilon_{ijk}\omega_k,\quad \Omega_{ij}=\overline{\Omega_{ij}}-\varepsilon_{ijk}\omega_k$$

Where; $\overline{\Omega_{ij}}$ is the mean rate-of-rotation tensor viewed in a moving reference frame with the angular velocity ω_k. The model constants A_0 and A_s are given by
A_0=4.04, $A_s=\sqrt{6}\cos\phi$
Where,

$$\phi=\frac{1}{3}\cos^{-1}\left[\sqrt{6}W\right],W=\frac{S_{ij}S_{ik}S_{ki}}{\tilde{S}^3},\tilde{S}=\sqrt{S_{ij}S_{ij}},S_{ij}=\frac{1}{2}\left(\frac{\partial u_j}{\partial x_i}+\frac{\partial u_i}{\partial x_j}\right) \tag{18}$$

It can be seen that C_μ is a function of the mean strain and rotation rates, the angular velocity of the system rotation, and the turbulence fields (k and ε).C_μ in Equation 16 can be shown to recover the standard value of 0.09 for an inertial sublayer in an equilibrium boundary layer.
The model constants C_2, σ_k and σ_ε have been established to ensure that the model performs well for certain canonical flows. The model constants are $C_{1\varepsilon}$=1.44, C_2=1.9, σ_k =1.0and σ_ε =1.2.

D. Computational domain

The size of computational domain depends on the region that shall be represented by the simulation [5]. Domain should be large enough to avoid reflecting of fluid streams, which may cause abnormal pressure fields around the model. For an accurate simulation, it is important to reproduce the influence of the surroundings as accurately as possible in the computational) being adhered to by workers when modelling low-rise buildings. For such low-rise buildings, where H-B-L (with B and L being the cross- and along wind

building dimensions respectively), these requirements produce domains that are both acceptable in physical and computational terms. By "acceptable in computational terms", it is meant that the domain boundaries are not so distant from the building that the number of computational cells required to fill the domain to ensure a reasonable level of accuracy becomes too large.
Various dimensions of the simulation volume are recommended in the literature:

(1) The blocking ratio should not exceed 3% [6]. The blocking ratio is the ratio between the buildings vertical surfaces exposed to the wind and the surface formed by the height and width of the simulated field which is generally the air inlet surface in the simulation.
(2) A blocking ratio less than 3% is recommended, even for large groups of buildings. The shape of the section of the simulation volume should preferably follow that of the buildings vertical surface exposed to the wind [5].
(3) The minimum length of the simulation field is 5 * min (L, 2H) upstream of the building and 8 * min (L, 2H) downstream of it, taking L equal to the length of the building and H equal to its height [7].
(4) The minimum dimensions of the simulation field are: 5H upstream of the building, 5H on each building side, 5H above it and 15 H downstream of the building. For a complex of buildings, the height H is the height of the highest building: Hmax [Hall 1997][8].

E. Boundary Conditions

Boundary conditions represent the influence of surroundings that have been cut off by the computational domain. The boundary conditions for inlet, outlet and outer walls should be provided. Various papers recommend the following boundary conditions for the simulation limits [Baetke et al 1990 ; Hall 1997 ; Blocken & al 2004 ; Francke & al 2004]:

(1) symmetries on the edges and the upper surface of the volume,
(2) "outflow" or a condition of zero pressure for the surface by which air leaves the simulation volume. The "outflow" boundary condition imposes a fully developed airflow at the exit, so it is important that the distance between building and exit is sufficiently long.
(3) a profile of wind speed varying with the height at the air entrance of the simulation field.

According to them, we used the symmetries and outflow boundaries for our simulations.
The inlet boundary conditions of the domain are defined by the vertical profile. The inlet wind vertical profile is represented in the power law profile form

$$U(z) = U_{ref}\left(\frac{z}{z_{ref}}\right)^{\alpha} \tag{19}$$

where, U(z) is the velocity at height z above the ground, Uref the basic wind speed at reference height, Z_{ref} the reference height above the ground, generally 10 m, and α is constant exponent power law, varying for different terrains.

F. Meshing

A good mesh requires great precision. The mesh should be highly refined at pedestrian level and in areas where strong wind gradients are planned. Adapting the mesh is an effective way to model accurately separation and attachment flow details without too many calculations [9].
With regard to the geometry of the region of interest, the computational grids that discretize the computational domain should be fine enough to provide an adequate resolution of the geometrical and expected flow features [10]. Generally, the greater the number of cells the better the CFD results, but as the number of cells increases, the calculation time also increases. The maximum number of cells that can be created for the solution depends on the computing resources available. According to the AIJ guidelines [Tominaga et al., 2008], the grid resolution must be at least 1/10 the building scale within the region that includes the evaluation points around the building of interest [11]. COST [Franke et al., 2007] also recommends a minimum of 10 cells per building side and at least 10 cells per cube root of building volume should be used for the initial grid resolution. To boost the accuracy of the simulation, local grid refinement can be used. Some commercial codes provide algorithms to adjust the local grid resolution according to numerical criteria obtained from the flow solution. However this accuracy comes at a cost, as any increase in the number of cells also increases the computer storage required and the run-time of the simulation. Thus, it is important to determine the optimum mesh size taking into account the available computer storage and run-time.
COST [Franke et al., 2007] suggests that grid stretching should be small in regions of high gradients, keeping the truncation error small. The shape of the grids can be categorized as either an unstructured or structured mesh. COST [Franke et al., 2007] consider hexahedral cells to be preferable to tetrahedral cells because hexahedral cells produce smaller truncation errors and provide better iterative convergence. They also note that when using tetrahedral cells, prismatic cells must be used at the wall and tetrahedral cells away from the wall since the grid lines should be perpendicular to the wall. Tominaga et al. [2008] also indicate that it is important to arrange that prismatic cells are parallel to walls and ground surfaces when using tetrahedral cells. Thus, both hexahedral and tetrahedral mesh can be used for CFD applications for wind flow around buildings. In addition, at least 10 cells per cube root of building volume are recommended for the initial grid resolution.

III. NUMERICAL SETUP

CFD code Fluent v17 is used to solve the 3D Reynolds-Average Navier-Stokes (RANS) equations and continuity equation, using the finite volume method. Standard k-ε model, RNG k-ε model and Realizable k- ε model with standard wall functions are used for turbulence modelling. SIMPLE algorithm is used for pressure-velocity coupling. As pressure based solver is used, second-order upwind discretization schemes are used for the convection terms and the viscous terms of the governing equations, i.e. conservation of mass and momentum equations.

IV. WIND FLOW AROUND A SINGLE BUILDING

In this study, the single high-rise building case is first considered. The building chosen for this work is a 1: 100 scale rectangular prism with a full scale size of 30.48 m (L)× 30.48 m (W) × 91.44 m (H). The arbitrary domain size shows in figure 1 to simulate the building within the atmospheric boundary layer. The dimensions of the computational domain are 518.16m × 274.32m×1097.28m in lateral, vertical and flow directions respectively.

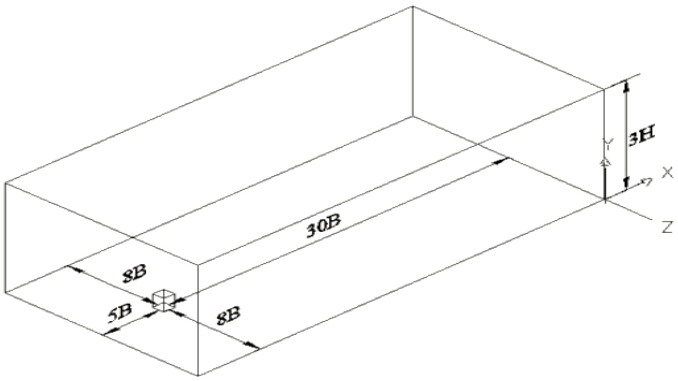

Figure 1: arbitrary domain size

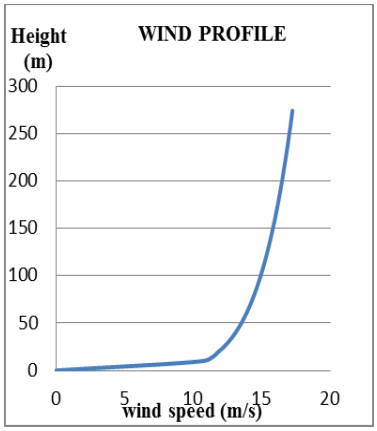

Figure 2: vertical profile for inlet boundary conditions

These dimensions respected a 1.96% blockage ratio (ratio of the front area of the building over the inlet area). Meshing is another important stage of a CFD simulation, which corresponds to accurate simulation of the atmosphere boundary layer as well as fluid motion near the ground. This mesh has over 1260000 nodes and over 1220000 elements by using MultiZone Meshing Method. The maximum cell size was 0.05m and minimum cell size was 0.001m. In this simulation, the aspect ratio of rectangular prism is 1:3 and the basic wind speed is considered 10.7535 m/s which are similar to the values simulated in the wind tunnel. The inflow wind velocity profile are computed by power law equation and imposed by UDF (C+ program). The vertical profile for inlet boundary condition is show in figure 2 and the summary of the data required for computation through ANSYS FLUENT is shown in Table 1.

Table .1: Input Parameter

S.N	Parameters	Values
1	Vertical Velocity Profile	$10.7535 \times (\frac{Z}{10})^{1/7}$
2	Basic Wind Speed (m/s)	10.7535
3	Power Law Coefficient, α	1/7
4	Turbulent Viscosity Ratio	10
5	Density of air (kg/m^3)	1.225
6	Viscosity of air (kg/m-s)	$1.7594*10^{-5}$
7	Solver	Pressure –based steady state
8	Models	standard k-ε model
9	Solution Method	SIMPLE pressure velocity coupling

A. SIMULATION RESULTS

Figure.3 is show the prediction of wind pressure distribution by simulation. The maximum wind pressure of the windward face of the building is 113.791 [pa], which are found two third of the building height. The minimum wind pressure of the building is -109.736 [pa] and is found at the corner of the building.

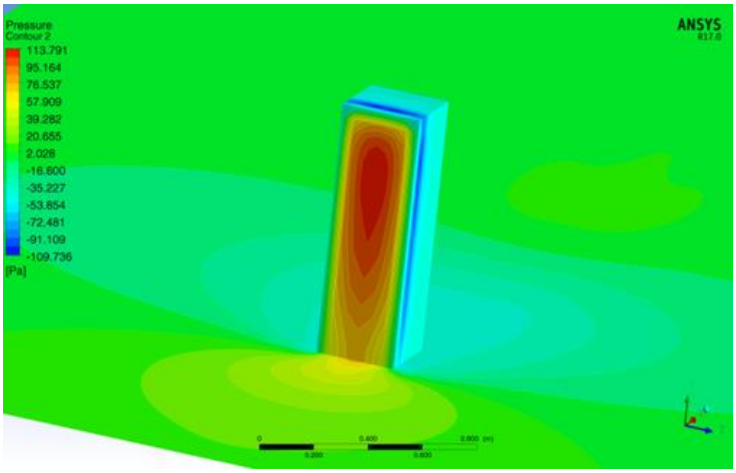

Figure 3: Contour Map of Pressure distributions

B. VALIDATION ON CFD SIMULATION

Figure 4 describes comparison of wind pressure coefficients on the windward wall obtained from this analysis and the experimental results obtained from TOKYO POLYTECHNIC UNIVERSITY "New frontier of Education and Research in Wind Engineering" for single high rise building case. The pressure coefficients follow a similar trend with the wind tunnel results on the windward wall. The results obtained in this research are matching with an average variation of 1% with wind tunnel result. Therefore, Computational fluid dynamics simulations programs are also very powerful tools for modeling the wind around buildings. They give a quantitative and qualitative wind flow representation of the whole volume simulated.

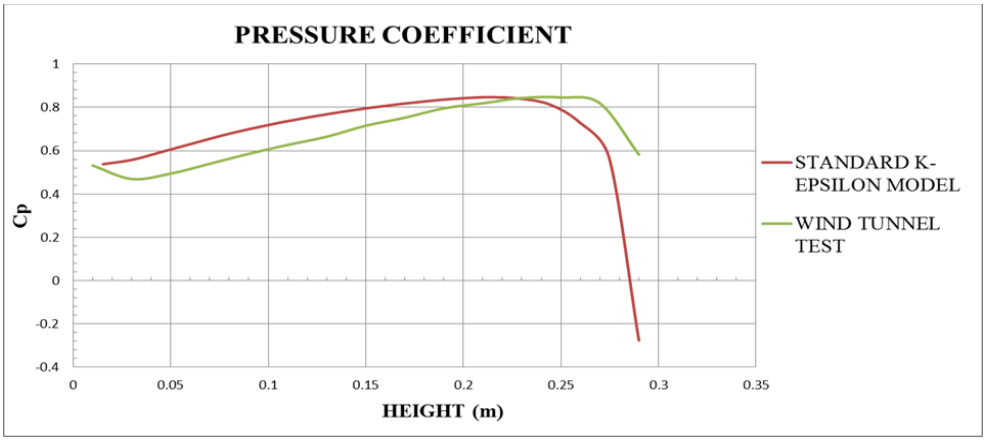

Figure 4: Comparison of pressure coefficients for the windward wall

V. WIND FLOW AROUND SURROUNDING BUILDINGS

Secondly, a high rise building with surrounding buildings cases are considered. A simple model with the urban area consider as arrays of identical building blocks with one high rise building in the center as show in figure 5. The target building has a size of 30.48 m (L)× 30.48 m (W) × 91.44 m (H) in full scale and the surrounding lower buildings have the same footprint with reduced height of 18.2888 m. figure 5a represents a single high-rise building and figure 5b describes target building with array one row lower buildings which have eight numbers of the building with the same height while figure 5c with target building with array two rows lower buildings which have twenty-four numbers of the building with the same height. The size of the computational domain, the value of input for boundary conditions and the numerical set up are similar with single building case.

Figure 5a: Single High Rise Buildings

Figure 5b: Target Building with Array One Row Lower Buildings

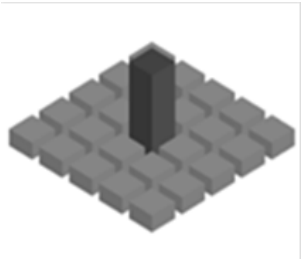

Figure 5c: Target Building with Array Two Rows Lower Buildings

A. SIMULATION RESULTS

The simulation results of wind pressure coefficient for (a) Single High rise Building (b) Target building with array one row lower buildings (c) Target building with array two rows lower buildings are shown in figure 6. For all three cases, it can be seen that the maximum wind pressure coefficient occurred to be at the middle of windward surface with height of about 0.73H and the minimum wind pressure coefficient generates at the corner of the flow separation. But, the single high rise building case is the highest value of wind pressure coefficient other than the two cases and the target building with array two rows surrounding buildings is the lowest value of wind pressure coefficient due to the sheltering effects around the building.

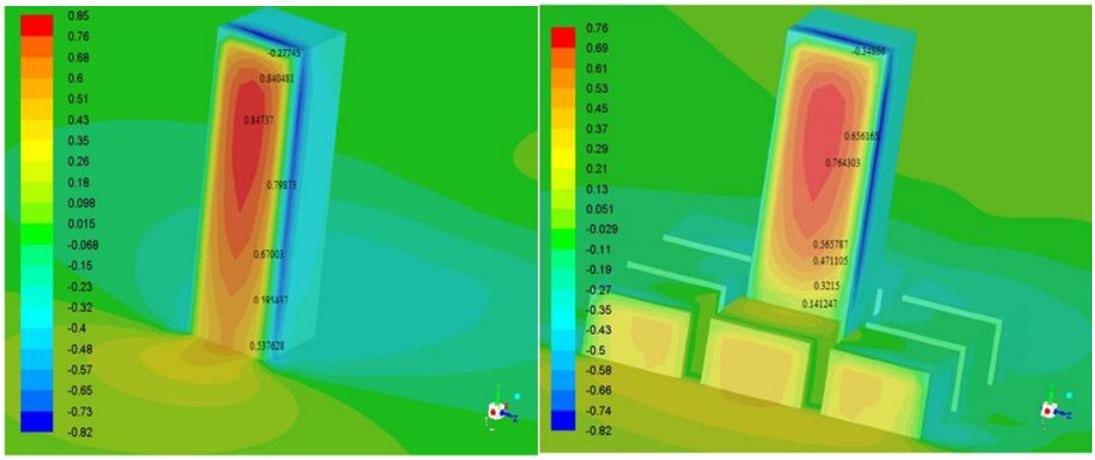

(a) (b)

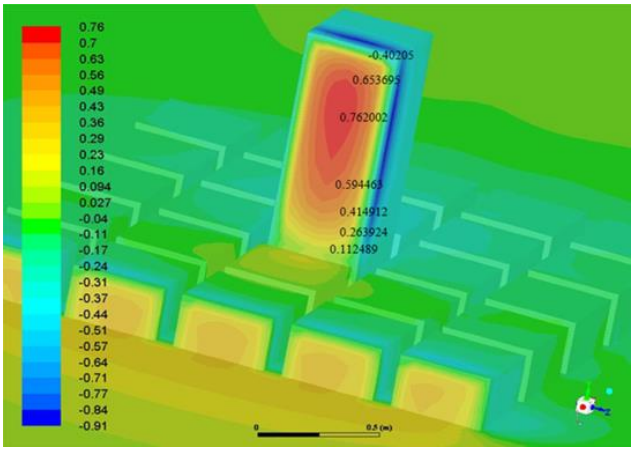

(c)

Figure 6: Comparison of pressure coefficient for (a) Single High rise Building (b) target building with array one row lower buildings (c) target building with array two rows lower buildings

VI. Wind Flow around Cluster of Existing Buildings

In this study, the arbitrary domain size is shown in figure 7 to simulate the building within the atmospheric boundary layer. The length of the simulation volume extends upstream of buildings over a distance of 5H, downstream over a distance of 20H, summaries side of the buildings over a distance of 5.5 H and height of the domain size over a distance of 5H, H being the height of the target building. The full scale dimensions of the computational domain are 571.15m × 228.5m×1236.3 in lateral, vertical and flow directions respectively. In this study, This mesh has over 2930000 nodes and over 285000 elements by using MultiZone Meshing Method. . The maximum cell size for all three domains was 0.02m and minimum cell size was 0.0001m.

In these simulation, the basic wind speed, U_{ref} , is 38.16 m/s in Mandalay from Myanmar National Building Code (2016) and exponent power law, α, is 1/7 for exposure categories B, urban and suburban areas, from ASCE 7-05. The vertical profile for inlet boundary condition is show in figure 8 and the summary of the data are similar with above the CFD simulation.

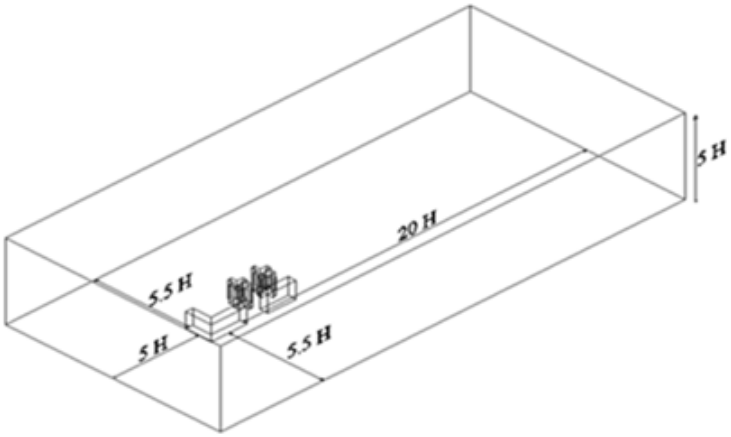

Figure 7: Arbitrary Domain Size

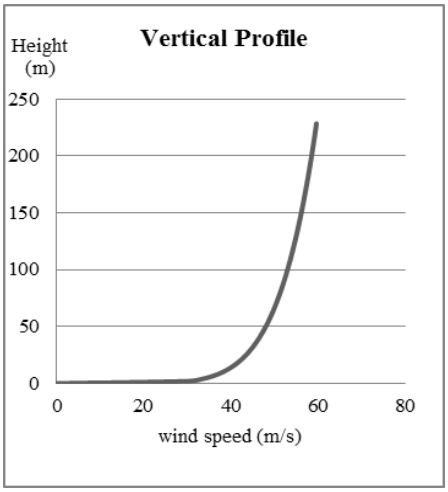

Figure 8: vertical profile for inlet boundary conditions

A. Simulation Results

To examine the airflow process, figure 9 and figure 10 demonstrate close up view of stream line pattern of the velocity on the horizontal plane at the middle height of the L-shape building and close up view of the pressure contours of wind field for directing the airflow (a) standard k-ε model, (b) RNG k-ε model and (c) Realizable k-ε model.

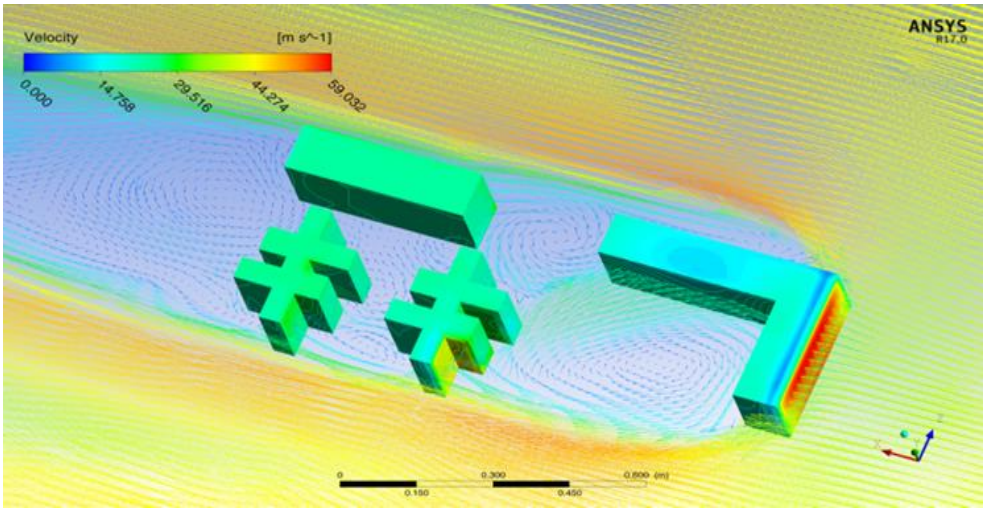

(a) standard k-ε model

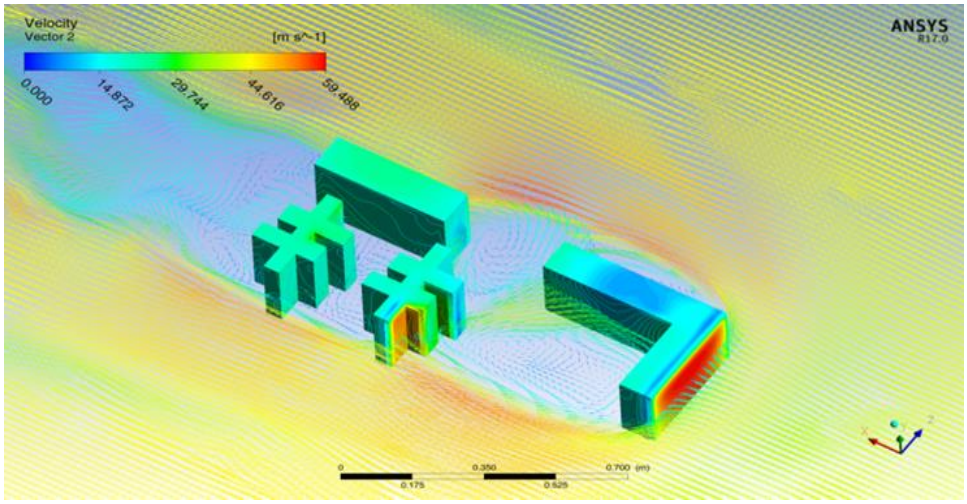

(b) RNG k-ε model

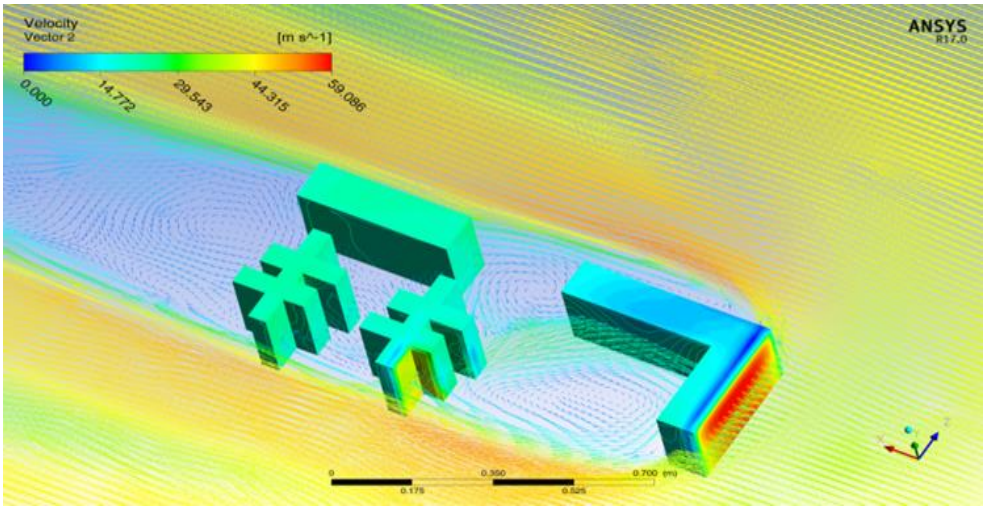

(c) Realizable k-ε model

Figure 9: Close up view of stream line pattern on the horizontal plane at the middle height of the L-shape building (a) standard k-ε model, (b) RNG k-ε model and (c) Realizable k-ε model

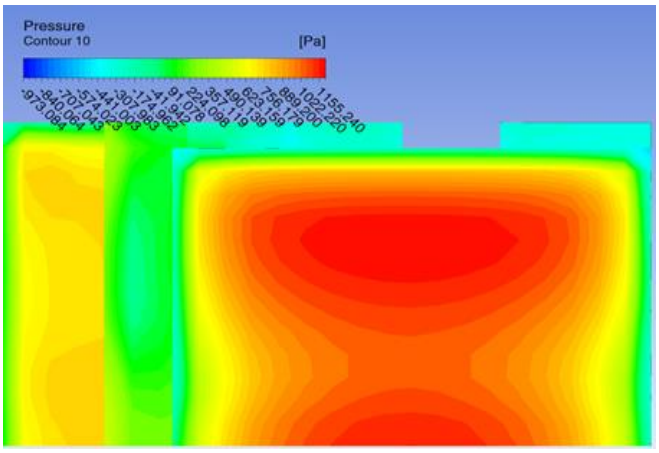

(a) standard k-ε model

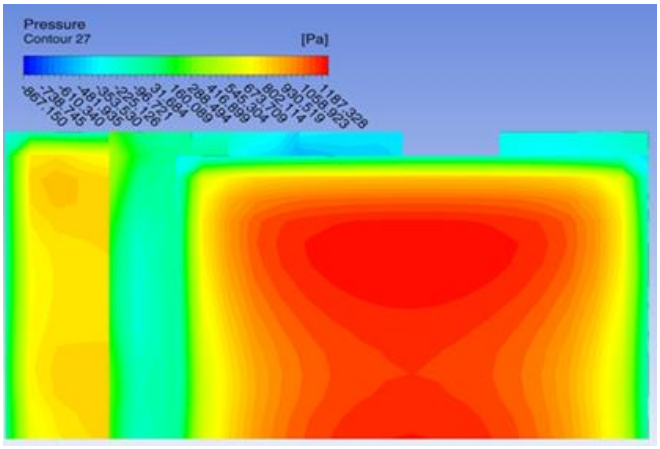

(b) RNG k-ε model

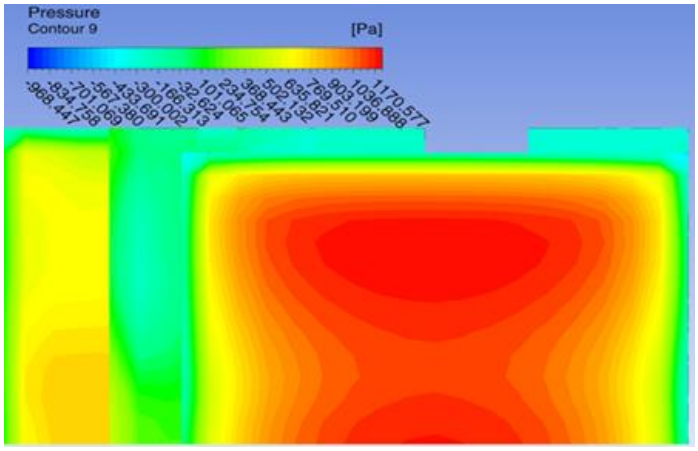

(c) Realizable k-ε model.

Figure 10: Close up view of the pressure contours of wind field for directing the airflow (a) standard k-ε model, (b) RNG k-ε model and (c) Realizable k-ε model.

It can be found that the Standard k-ε model and Realizable k-ε model predict similarly the magnitude of the maximum velocity while the RNG k-ε model is the most value of the maximum velocity other than two models. The Standard k-ε model and Realizable k-ε model appear to produce exactly prediction wake recirculation zone. The RNG k-ε model greatly over predicts the size of the recirculation zone and a strong wake flow among buildings. The standard k-ε, RNG k-ε, realizable k-ε models produce similarly shaped contour map of pressure but with significant differences in magnitude. For three different turbulent models, the maximum wind pressure are obtained 1197.63, 1230.13, 1217.15 [pa] and the minimum pressure are obtained -958.755, -867.15, -948.491[pa], respectively.

The comparison of pressure coefficients for the windward wall of the L-shape building with different turbulent model demonstrated in figure 11.

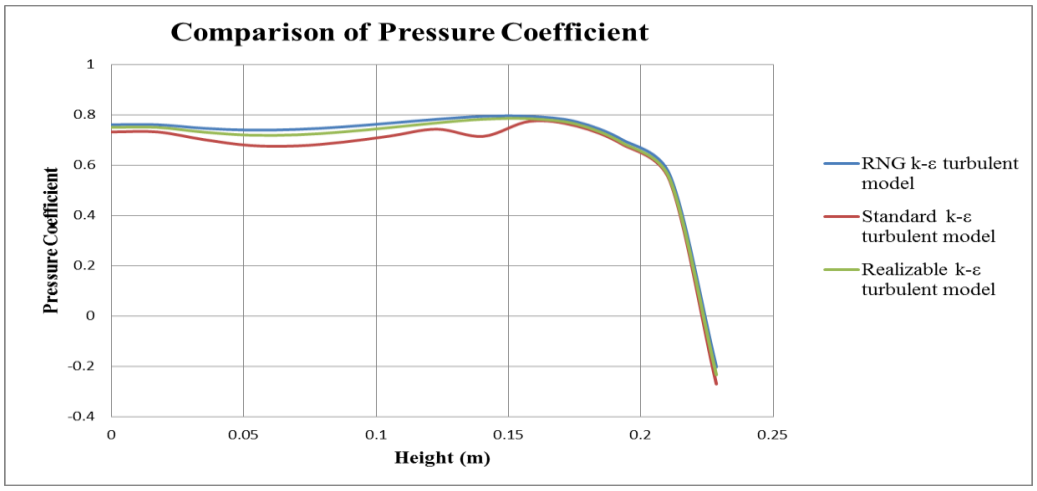

Figure 11: Comparison of pressure coefficients for the windward wall of the L-shape building with different turbulent model

It can be easily found that in three turbulence models, RNG k-ε model is the highest pressure coefficient other than turbulence models. The maximum wind pressure coefficients of the windward wall of the L-shape building with different turbulent model are 0.79, 0.77, 0.78, respectively, which are close to the value of 0.8 stipulated in the Myanmar National Building Coad.

VII. CONCLUSION

Applying the CFD as an effective tool to simulate the urban wind flowing across the neighborhood, city planners can better understand a conceivable physical environment of the urban areas with the predicted streamlines, velocity and pressure distribution at the pedestrian level. This journal has presented a CFD simulation for the evaluation of wind pressure coefficient and safety in urban areas, the use of CFD solutions related to environmental concerns has been demonstrated through three case studies.

We considered a special case of urban area with a high-rise building in the center surrounded by multiple layers of identical lower

buildings to understand the sheltering effect of the surroundings on the surface wind pressure distribution, which is needed for natural ventilation design and optimizing design. The more layers of the surrounding buildings, the less surface pressure coefficients on the target building. The maximum wind pressure coefficient occurred to be at the middle of windward surface with height of about 0.73H and the minimum wind pressure coefficient generates at the corner of the flow separation. Vortices occur in both windward and leeward sides of the L-shape building and inside the surrounding buildings. In the center of these vortices, the suction is large, possibly leading to structural severe damage. Among three different models, the Realizable k- ε model is the most suitable model for numerical simulation of wind flow around building in ANSYS Fluent.

ACKNOWLEDGMENT

The author wishes to express her deepest gratitude to her Excellency, Union Minister Dr. Myo Thein Gyi, Ministry of Education in Myanmar.

The author is deeply gratitude to Dr. Sint Soe, Rector, Mandalay Technological University, for his kindness, help, permission, guidance and advice of this paper.

The author would like to thank to Dr. Nilar Aye, Professor, Head of Department of Civil Engineering, Mandalay Technological University, for her valuable suggestion and giving useful comments.

The author owes a debt of gratitude to her supervisor, Dr. Sun Yu Khaing, Professor of the Department of Civil Engineering, Mandalay Technological University, for her enthusiastic instruction, invaluable help, and indispensable guidance in the preparation of this paper.

Finally, the author wishes to express her heartfelt thanks to her family, especially her parents and all other persons for their supports and encouragements to attain her destination without any trouble.

REFERENCES

[1] S., Bungale, Taranath, Wind and Earthquake Resistant Buildings, 2005.

[2] Daeung Kim, (2013, December 11), "The Application of CFD to Building Analysis and Design: A Combined Approach of an Immersive Case Study and Wind Tunnel Testing'' Architecture and Design Research, Blacksburg, Virginia.

[3] Garatt, J. R., Hess, G. D., Physick, W. L, Bougeault, P., The Atmospheric Boundary Layer – Advances in Knowledge and Applications, Boundary Layer Meteorology, 78, pp 9 – 37, 1996.

[4] Ismail B. Celik, (1999, December), "Introductory Turbulence Modeling" Mechanical & Aerospace Engineering Dept, West Virginia University, P.O. Box 6106, Morgantown, WV 26506-6106.

[5] J., Franke, Recommendations of the Cost Action c14 on the use of CFD in Predicting Pedestrian Wind Environment. In: the 4th International Symposium on Computational Wind Engineering, Japan Association for Wind Engineering, 2006.

[6] F., Baetke, H., Warner, (1990), Numerical Simulation of Turbulent Flow over Surface Mounted Obstacle with Sharp Edges and Corners, Journal of Wind Engineering and Industrial Aerodynamics, 1990.

[7] B., Blocken, J., Carmeliet, T., Stathopoulos, CFD Evaluation of the Wind Speed Conditions in passages between Buildings- Effect of Wall-function Roughness Modifications on the Atmosphere Boundary Layer Flow. Journal of Wind Engineering and Industrial Aerodynamics, 2007.

[8] H, K., Veersteeg, W., Malalasekara, W., An Introduction to Computational Fluid Dynamic, Prentice Hall,1995.

[9] MERONEY Robert N., LEITL Bernd M., RAFAILIDIS Stillianos, SCHATZMANN Michael, Wind-tunnel and numerical modelling of flow and dispersion about several building shapes, Journal of Wind Engineering and Industial Aerodynamics, 81, 1999, 333-345, Elsevier.

[10] Casey, M., & Wintergerste, T. (2000). Best Practice Guidelines, ERCOFTAC Special Interest Group on Quality and Trust in Industrial CFD. ERCOFTAC, Brussels.

[11] Y., Tominagaa, A., Mochida, M.,Yoshikawa, T., Shirasawa, AIJ Guidelines for Practical Applications of CFD to Pedestrain Wind Environment around Buildings, Journal of Wind Engineering and Industrial aerodynamics ,2008.

AUTHORS

First Author – That Mon Soe, Ph.D Student, Mandalay Technological University, thetmonsoe.658@gmail.com
Second Author – San Yu Khaing, Professor, Mandalay Technological University, sykpuk@gmail.com